JVI Journals.ASM.org

Stabilizing the Native Trimer of HIV-1 Env by Destabilizing the Heterodimeric Interface of the gp41 Postfusion Six-Helix Bundle

Sannula Kesavardhana,[a] Raghavan Varadarajan[a,b]

Molecular Biophysics Unit, Indian Institute of Science, Bangalore, India[a]; Jawaharlal Nehru Centre for Advanced Scientific Research, Jakkur, Bangalore, India[b]

ABSTRACT

The HIV-1 envelope glycoprotein (Env) is a trimer of gp120-gp41 heterodimers and is essential for viral entry. The gp41 subunit in native, prefusion trimeric Env exists in a metastable conformation and attains a stable six-helix bundle (6-HB) conformation comprised of a trimer of N-heptad repeat (NHR) and C-heptad repeat (CHR) heterodimers, that drives the fusion of viral and cellular membranes. We attempted to stabilize native Env trimers by incorporation of mutations at the NHR-CHR interface that disrupt the postfusion 6-HB of gp41. The mutations V570D and I573D stabilize native Env of the HIV-1 JRFL strain and occlude nonneutralizing epitopes to a greater extent than the previously identified I559P mutation that is at the interface of the NHR trimers in the 6-HB. The mutations prevent soluble-CD4 (sCD4)-induced gp120 shedding and 6-HB formation. In the context of cell surface-expressed JRFL Env, introduction of a previously reported additional disulfide between residues A501 and T605 perturbs the native conformation, though this effect is partially alleviated by furin coexpression. The data suggest that positions 570 and 573 are surface proximal in native Env and that the NHR homotrimeric coiled coil in native Env terminates before or close to residue 573. Aspartic acid substitutions at these positions stabilize native trimers through destabilization of the postfusion 6-HB conformation. These mutations can be used to stabilize Env in a DNA vaccine format.

IMPORTANCE

The major protein on the surface of HIV-1 is the envelope (Env) glycoprotein. Env is a trimer of gp120-gp41 heterodimers. gp120 is involved in receptor/coreceptor binding and gp41 in the fusion of viral and cellular membranes. Like many other viral fusion proteins, the gp41 subunit in native trimeric Env exists in a metastable conformation. gp41 readily forms a stable six-helix bundle (6-HB) conformation comprised of a trimer of N-heptad repeat (NHR) and C-heptad repeat (CHR) heterodimers that drives fusion of viral and cellular membranes. While it is expected that native Env is a good immunogen, its metastability results in exposure of immunodominant nonneutralizing epitopes. In the present study, we stabilize native Env trimers by incorporation of a number of different mutations at the NHR-CHR interface that disrupt the postfusion 6-HB of gp41. The stabilized constructs described here can be incorporated into DNA vaccine candidates.

The HIV-1 envelope glycoprotein (Env) is synthesized as a gp160 precursor protein that is cleaved into surface-exposed gp120 and membrane-anchored gp41 subunits. The gp120 and gp41 subunits associate noncovalently to make a functional trimeric envelope spike on the virion surface (1, 2). Trimeric Env is essential for host cell recognition and subsequent membrane fusion. During the process of fusion, the envelope spike samples different conformations to achieve fusion of cellular and viral membranes. Binding of gp120 to CD4 induces structural rearrangements in Env and results in an active, open, quaternary conformation where gp120 subunits move apart and the coreceptor binding site on gp120 is exposed (3). Binding of coreceptor (CCR5/CXCR4) leads to the formation of a pre-hairpin intermediate and gp120 shedding, followed by stable gp41 six-helix bundle (6-HB) formation. Native unliganded Env is known to be unstable on the virion surface, as the membrane-bound gp41 subunit in the trimer exists in a metastable conformation that eventually transforms into a stable 6-HB conformation following fusion (4).

Env protein is the primary target for vaccine design because it is surface accessible and an essential molecule for HIV-1 entry (1). In HIV-1 infection, viruses elicit largely Env-directed antibodies, but with limited neutralization capacity (5). The low neutralization potency is due in part to immunodominant epitopes in shed gp120 and unprocessed Env on the virus surface (6, 7). Combined with a high mutational rate and extensive glycosylation, this facilitates immune evasion (8, 9). The structure of monomeric gp120 has been determined in its unliganded and ligand-bound states (8, 10). It has been shown that vaccine candidates based on monomeric gp120 are poor immunogens that have so far failed to elicit a protective immune response against HIV-1 (11, 12). Monomeric-gp120-based immunogens elicit antibodies that typically protect against infection with homologous or easy-to-neutralize tier 1 viral isolates (12, 13). A recently completed RV144 clinical trial study, where monomeric gp120 (a combination of subtypes B/E) was used as a vaccine candidate, showed ~31.2% efficacy and is the most encouraging HIV-1 vaccine trial to date (14). Though sera from the RV144 clinical trial did not neutralize circulating viruses (15), the vaccine still confers partial protection.

Trimeric Env immunogens are thought to be better immuno-

Received 17 February 2014 **Accepted** 2 June 2014

Published ahead of print 11 June 2014

Editor: G. Silvestri

Address correspondence to Raghavan Varadarajan, varadar@mbu.iisc.ernet.in.

Supplemental material for this article may be found at http://dx.doi.org/10.1128/JVI.00494-14.

doi:10.1128/JVI.00494-14

gens than monomeric gp120. Native trimeric Env expressed on the HEK 293T cell surface bound neutralizing antibodies (NAbs) efficiently, whereas nonneutralizing antibodies did not bind or bound weakly (16). Previous reports suggested that the gp120 conformation in the context of the Env spike is the structure recognized by many neutralizing antibodies. Quaternary epitope-specific neutralizing antibodies bind to gp120 in its trimeric Env context with much higher affinity than the corresponding monomeric form (17, 18). A major obstacle in HIV-1 vaccine research is the lack of an atomic resolution structure for the native Env trimer. Recently, the cryo-electron microscopy (cryo-EM) and crystal structures of trimeric disulfide-stabilized gp140 were determined (19–21). While these produce valuable information on the relative orientations of the gp41 N-heptad repeat (NHR) and C-heptad repeat (CHR) and gp120, no side chain coordinates for gp41 are present in these structures. Although native trimeric Env is believed to be a better immunogen than monomeric gp120 (22), the design and purification of Env glycoprotein in its native trimeric form is difficult and challenging due to the instability and misfolding of the purified functional HIV-1 Env trimer.

Various approaches have been explored to design trimeric Env immunogens in which the protease cleavage site between gp120 and gp41 was mutated so that the two subunits remained covalently linked (23, 24). In an alternative approach, a disulfide bond was introduced between gp120 and gp41 (25–28). The trimeric immunogen candidates designed so far have failed to elicit antibodies that can neutralize diverse HIV-1 isolates, although there is some improvement in eliciting neutralizing antibodies relative to monomeric gp120 (29). Thus, the design and purification of native-like Env trimers is an important problem in HIV-1 vaccine development. Lack of a high-resolution native trimeric Env crystal structure, weak noncovalent interaction between gp120 and gp41 subunits, and a metastable conformation of Env hinder the design of native-like trimeric Env immunogens.

In the present study, we designed and characterized mutations that destabilize the stable postfusion conformation of gp41 and examined the stability of Env in the presence of such 6-helix bundle-destabilizing (6-HBD) mutations. Mammalian cell surface display of HIV-1 Env trimers was used to probe the conformational changes of the native Env trimer in the presence of 6-HBD mutations. Mutating residues present at the interface of the N-heptad and C-heptad repeat regions of the 6-HB conformation of gp41 prevented postfusion six-helix bundle formation and retained the conformational integrity of the native Env trimer. These 6-HBD mutations prevent soluble-CD4 (sCD4)-induced gp120 shedding, presumably by stabilizing the native conformation of Env. We anticipate that this information can be used to design improved trimeric immunogens and can also be incorporated into DNA vaccine constructs.

MATERIALS AND METHODS

Constructs. REJO, DU156, ZM109, SF162, and DU422 Env clones were obtained from the NIH AIDS Reagent and Reference Program, Division of AIDS, NIAID, NIH. The REJO, DU156, SF162, and DU422 Env genes were expressed from the pcDNA3.1 plasmid, and the ZM109 Env gene was expressed from the pCR3.1 plasmid. The pSVIII-JRFL gp160dCT plasmid encodes envelope glycoprotein with a cytoplasmic tail truncated at residue 711. The HIV-1 strain JRFL gp160dCT gene in this plasmid is the non-codon-optimized viral sequence. The pctat expression plasmid encodes the HIV-1 tat protein. I559P, V570D, I573D, and S649D mutations were introduced individually into the JRFL gp160dCT background to make gp160-I559P, gp160-V570D, gp160-I573D, and gp160-S649D by site-directed mutagenesis. Also, I559P and V570D mutations were introduced into pCDNA3.1-DU422 Env by site-directed mutagenesis. A501C and T605C mutations were introduced into pSVIII-JRFLgp160dCT by site-directed mutagenesis to make gp160-SOS. In the gp160-SOS background, I559P or V570D mutations were introduced to make gp160-SOSIP or gp160-SOS-V570D constructs. The E168K mutation was introduced into gp160dCT and gp160-V570D to make gp160-E168K and gp160-V570D-E168K constructs for PG9 and PG16 binding studies. The E168K mutation was previously shown to confer PG9/PG16 binding on JRFL Env. This mutation was also introduced into gp160-SOSIP and gp160-SOS-V570D. To make JRFL gp160 cleavage defective, the gp120-gp41 cleavage site region REKR was mutated to SEKS by site-directed mutagenesis. In another construct, to enhance the cleavage efficiency of gp160, we replaced the cleavage site (REKR) with six arginine residues (R6) to make gp160dCT-R6-E168K. Previous studies showed that replacement of the REKR cleavage site with R6 improved the cleavage of gp160 to gp120 and gp41 (30). Unless otherwise stated, all mutations were made in the background of the JRFL Env sequence. Residue numbering follows the conventional HXBc2 numbering scheme.

Transient transfection of Env plasmids. One day prior to transfection, 3×10^6 293T cells were seeded in a T75 culture flask. After 24 h, the cells were transfected with pSVIII JRFL gp160dCT expression plasmids encoding wild-type (wt) Env and 6-HBD mutants. In all cases, the tat expression plasmid (pctat) was cotransfected using Polyfect (Qiagen) transfection reagent unless otherwise stated. The cells were harvested 48 h after transfection for analysis.

Staining of cell surface-expressed Env for FACS analysis. After 48 h of transfection, the cells were harvested with phosphate-buffered saline (PBS) (pH 7.4) containing 5 mM EDTA and washed with fluorescence-activated cell sorter (FACS) buffer (PBS, 5% fetal bovine serum, and 0.02% azide). The harvested cells (4×10^5 cells per tube) were stained with the desired antibody for 1 h at 4°C. The antibody-cell mixture was washed in FACS buffer, and anti-human IgG phycoerythrin (PE) (Sigma) at 1:100 dilution was added and incubated for 1 h at 4°C. The cells were washed again with FACS buffer before analysis. Anti-rabbit IgG-PE (Sigma) at 1:100 dilution was used for labeling when cells were stained with anti-gp120 rabbit polyclonal sera and anti-mouse IgG-PE for D49 antibody-stained cells. The stained cells were analyzed on a FACS analyzer (BD FACSCantoII or BD Accuri).

After harvesting, cell viability was determined by the trypan blue dye exclusion method. A cell viability test was done prior to each FACS experiment for accurate determination of cell membrane integrity, and the result was typically >80%. The cells were gated on forward scatter and side scatter (FSC-SSC) plots to discriminate between dead cells, doublets, and live or single cells. The mean fluorescence intensity (MFI) values were obtained from the gated single-cell population. In each experiment, unstained controls, secondary-antibody controls, and untransfected cells with primary- and secondary-antibody controls (Fig. S4) were prepared in parallel with test samples. Each FACS experiment was repeated independently (with independent transfection experiments) to check for consistency of results. BD FACS-Diva, BD Accuri, and FlowJo software was used to analyze the data and to obtain statistical information.

sCD4-induced gp120 shedding experiments. (i) ELISA. After 48 h of transfection, cells were harvested and washed with FACS buffer. The harvested cells (1×10^6 cells per tube) were incubated in the presence and absence of sCD4 (four-domain sCD4, obtained from the Neutralizing Antibody Consortium [NAC]) at various concentrations for 2 h at 4°C with occasional mixing of samples. The cells were centrifuged at $210 \times g$ for 2 min, and the supernatant containing shed gp120 was collected. Each well of a 96-well enzyme-linked immunosorbent assay (ELISA) plate (Nunc) was coated with 200 ng of gp120-capturing antibody (D7324) overnight at 4°C. Supernatants containing shed gp120 were added to these D7324-coated plates and incubated for 1 h at room temperature. After 1 h, the wells were washed four times with PBS, 0.025% Tween 20 (PBST) four

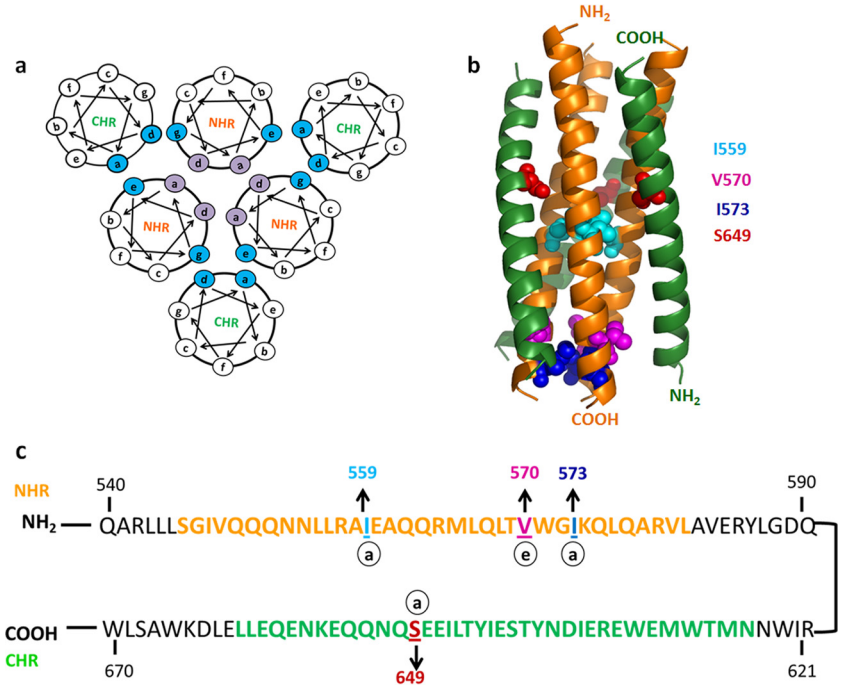

FIG 1 Six-helix bundle-destabilizing mutations. (a) Helical-wheel diagram of postfusion 6-HB. Residues essential for NHR trimer formation (purple) and residues essential for CHR interaction with NHR to form 6-HB (cyan) are highlighted. (b) Postfusion six-helix bundle of gp41 (Protein Data Bank [PDB] ID, 3CP1) generated using PYMOL (PYMOL molecular graphics system version 1.2r2; DeLano Scientific, LLC). Residues mutated for 6-HB disruption are represented in space-filling mode. The NHR region is shown in orange and the CHR region in green. (c) Sequences of NHR and CHR regions from the JRFL gp41 subunit. Residues individually mutated to disrupt 6-HB formation are highlighted. The NHR region is highlighted in orange, and the CHR region is highlighted in green.

times. To detect captured gp120, 2G12 antibody was added and incubated for 1 h at room temperature. Samples were washed again, and anti-human IgG antibody conjugated to alkaline phosphatase (Sigma) was added and incubated at room temperature for 1 h. After a wash, developing solution (*p*-nitrophenyl phosphate; Sigma) was added, and the absorbance was measured at 410 nm using a Spectramax Plus 384 (Molecular Devices, USA).

(ii) FACS. After 48 h of transfection, cells were harvested and washed with FACS buffer. The harvested cells (1×10^6 cells per tube) were incubated with or without sCD4 at 50-μg/ml concentration for 2 h at 4°C with occasional mixing. To remove shed gp120, the cells were washed with FACS buffer. Then, the cells were incubated with either 2G12 antibody or D49 antibody at various concentrations for 1 h at 4°C. After a wash, the cells were incubated with anti-human IgG-PE (Sigma) to stain 2G12 antibody-bound cells and with anti-mouse IgG-PE (Sigma) to stain D49 antibody-bound cells. After a wash, the cells were analyzed on a FACS analyzer (BD Canto or BD Accuri). BD FACS-Diva 6.1.3 and BD Accuri software was used to analyze the data.

SPR experiments. Surface plasmon resonance (SPR) experiments were performed with a Biacore 2000 (Biacore, Uppsala, Sweden) optical biosensor at 25°C. Briefly, ~800 resonance units (RU) of b12 and b6 antibodies were immobilized by amine coupling to the surface of a CM5 chip. The binding of DU422 gp120 to these antibodies was examined. DU422 gp120 was passed across each sensor surface at different concentrations.

Western blot analysis. The cells were harvested after 48 h of transfection, and the harvested cells (3×10^6) were subjected to cell lysis in 200 μl cell lysis buffer (10 mM Tris, 0.15 M NaCl, 1% NP-40 detergent, protease inhibitor cocktail, pH 8) for 1 h on ice. The lysed cells were centrifuged at 15,000 × *g* for 30 min. The cell lysates were separated from cell debris and stored at −80°C till further use. Forty microliters of cell lysate from each transfection was subjected to SDS gel electrophoresis and then transferred to a nitrocellulose membrane to probe with rabbit anti-gp120 polyclonal serum (1:1,000 dilution). The blots were labeled with anti-rabbit IgG-peroxidase (Sigma) at 1:5,000 dilution and developed with enhanced chemiluminescence (ECL) substrate to detect Env proteins.

RESULTS

Expression of trimeric Envs from various different HIV-1 subtypes. Using a yeast surface two-hybrid (YS2H) system, we previously succeeded in reconstituting the postfusion six-helix bundle of HIV-1 gp41 on the yeast surface by expressing the NHR from gp41 as a membrane-anchored prey and the CHR as a secretory bait (31). This system allowed us to rapidly characterize mutations destabilizing 6-HB formation. The 6-HB consists of a central NHR trimer with a CHR peptide bound to each NHR (4). Mutations to disrupt helix-helix interactions in the 6-HB involved either mutations disrupting NHR trimer formation or those involved in interactions between the NHR and the CHR. Among various mutations screened previously (31) the I559P, V570D, I573D, and S649D mutations destabilized six-helix bundle formation on the yeast surface (Fig. 1). In the present study, we examined the effects of 6-HBD mutations on Env trimer stability and integrity.

Earlier studies have shown that when JRFL gp160 truncated at its cytoplasmic tail (JRFL gp160dCT) is expressed on the HEK 293T cell surface, gp160 is efficiently processed into gp120 and gp41, and native-like Env oligomers are displayed on the cell surface (16, 32, 33). These cleaved, surface-expressed Env oligomers were probed for binding to neutralizing and nonneutralizing antibodies by FACS. Properly cleaved native Env trimers bind

selectively to CD4 binding site (CD4bs)-directed neutralizing antibodies, such as b12, but not to corresponding nonneutralizing antibodies, such as b6 and F105, as well as other nonneutralizing antibodies specific to different regions of Env (16). However, uncleaved Env (JRFL gp160-SEKS) on the cell surface bound equally well to both b12 and b6 and also showed significant binding to other nonneutralizing antibodies. In addition to this, previous reports showed that HIV-1 JRFL Env glycoprotein expressed on the cell surface by transient transfection is oligomeric and predominantly trimeric (34). Hence, we used FACS combined with cell surface expression to characterize mutations that selectively destabilize the postfusion six-helix bundle, but not native trimeric Env.

We initially characterized cell surface expression of Env from various subtypes to select an HIV-1 Env that is well displayed on the cell surface. Various Env glycoproteins from clade B (SF162, REJO, and JRFL) and clade C (DU156, ZM109, and DU422) HIV-1 strains were expressed on the HEK 293T cell surface individually. SF162, REJO, DU156, ZM109, and DU422 Env clones are full-length Env plasmids. In the JRFL Env clone, the Env gene was truncated at the cytoplasmic tail (35). The JRFL Env expression level was higher than those of other strains, possibly because of this truncation. Apart from expression levels, cell surface expression allowed us to compare Env integrity. To examine native Env integrity, Env-expressing cells were stained with CD4bs-directed neutralizing and nonneutralizing antibodies. Properly cleaved trimeric Env efficiently binds neutralizing antibodies but not nonneutralizing antibodies. Forty-eight hours after transfection, cells were harvested and stained with CD4bs site neutralizing (b12) and nonneutralizing (b6) antibodies to screen for an Env that was cleavage competent and native-like based on the previously established FACS method (16). Clade B isolates bound more efficiently to neutralizing (b12) than to nonneutralizing (b6) antibodies (see Fig. S1a in the supplemental material). JRFL Env showed the largest difference between neutralizing- and nonneutralizing-antibody binding (~6-fold), which indicates good display of cleavage-competent trimeric Env on the cell surface (see Fig. S1b in the supplemental material). In the case of clade C isolates, DU422 Env showed a measurable difference between b12 and b6 antibody binding. JRCSF and YU2 subtype Envs also exhibited less discrimination than JRFL in b12 and b6 antibody binding patterns (16, 17). Recent studies also suggest that Env glycoprotein from HIV-1 JRFL is homogeneous and trimeric (36). Thus, in further experiments, we chose JRFL-Env glycoprotein for characterizing 6-HBD mutations in the context of native Env trimers and confirmed the generality of the observations by studying the effects of identical mutations in DU422 Env.

Antigenicity profiles suggest that most 6-HBD mutations did not perturb the native conformation. The previously characterized six-helix bundle-destabilizing mutations (I559P, V570D, I573D, and S649D) disrupt six-helix bundle formation in a yeast surface two-hybrid system (31). These mutations were introduced individually into non-codon-optimized JRFL gp160 (truncated at its cytoplasmic tail) in order to stabilize trimeric Env in a native-like conformation by disrupting six-helix bundle formation. Destabilizing six-helix bundle formation in gp41 might be expected to stabilize gp41 in its native conformation, since formation of the 6-HB is an irreversible step that prevents reformation of the native gp120-gp41 trimer. We have previously used a similar strategy to stabilize the stem domain of hemagglutinin in influenza virus in its native conformation (37, 38). The previously described mutations to make Env cleavage defective (REKR to SEKS) were also introduced into non-codon-optimized JRFL gp160 (16, 39). To study the effects of mutations on trimer integrity, HEK 293T cells were cotransfected with each of the gp160 mutants, along with a tat expression plasmid. The cells were harvested after 48 h and processed for FACS analysis to examine binding to various gp120- and gp41-directed antibodies. The overall level of Env surface expression was probed with mannose-specific 2G12 monoclonal antibody. The MFIs from FACS histograms were plotted as a function of the antibody concentration to generate binding curves.

The cells transfected with wt gp160 and six-helix bundle-destabilizing mutants (gp160-V570D and gp160-I573D) bound neutralizing antibody b12 more efficiently than the nonneutralizing antibody b6 (~5- to 6-fold difference) (Fig. 2a and b). However, the gp160-I559P mutant showed less binding to b12 than wt gp160 and gp160-V570D, and the discrimination between b12 and b6 binding was significantly less for I559P than for wt gp160, gp160-V570D, gp160-I573D, and gp160-S649D ($P < 0.05$, using a two-tailed unpaired t test at an antibody concentration of 10 μg/ml) (Fig. 2b). gp160-S649D also behaved similarly to wt gp160 in relative b12 and b6 antibody binding patterns, though the binding MFIs were lower (Fig. 2a). Cleavage-defective Env (JRFL gp160-SEKS) bound equally well to b12 and b6, as reported previously (16) (Fig. 2). In all Env 6-HBD mutants, the b12 epitope conformation is retained. These data suggest that V570D, I573D, and S649D mutations in Env did not perturb the CD4bs epitope, whereas I559P may have altered the native structure or cleavage efficiency of JRFL Env. The cell surface expression levels of all constructs were probed with 2G12 antibody and were found to be approximately comparable, though wt gp160 showed slightly better expression than the mutants (see Fig. S3 in the supplemental material). Binding studies with other gp120-specific nonneutralizing antibodies (C11 and 17b) were also carried out. Both antibodies bound significantly better to cleavage-defective Env than to wild-type and 6-HBD mutant Env (see Fig. S2 in the supplemental material). 17b binds to Env following CD4 binding. Hence, its epitope is referred to as a CD4-induced (CD4i) epitope. When incubated with soluble CD4 for a short time, all 6-HBD mutants bound to 17b (data not shown). To extend these observations to a subtype C HIV-1 isolate, I559P and V570D mutations were introduced into DU422 Env. When probed with different NAbs and nonneutralizing antibodies, results similar to those for JRFL were observed (Fig. 3).

To demonstrate the effect of Env cleavage on the FACS binding pattern of neutralizing (b12) and nonneutralizing (b6) antibodies, we performed Western blot analysis of Env glycoproteins expressed on HEK 293T cells. Cell lysates from cleavage-defective Env (gp160-SEKS)-expressing cells showed unprocessed gp160, as expected (see Fig. S2 in the supplemental material). As previously reported, there are two different gp160 species in cleavage-defective Env cell lysates (16). The higher-molecular-weight species is the hyperglycosylated gp160, which is a predominant form of uncleaved Env (16). In cell lysates from wt gp160 (gp160-REKR)-expressing cells, most of the fraction is gp120, which is the product of gp160 cleavage, though residual uncleaved gp160 was observed (see Fig. S2 in the supplemental material). This indicates that wt gp160 is efficiently cleaved and is displayed on the cell surface. Thus, inefficient cleavage of gp160-SEKS allowed binding of both b12 and b6 antibodies equally well, while efficient cleavage of wt

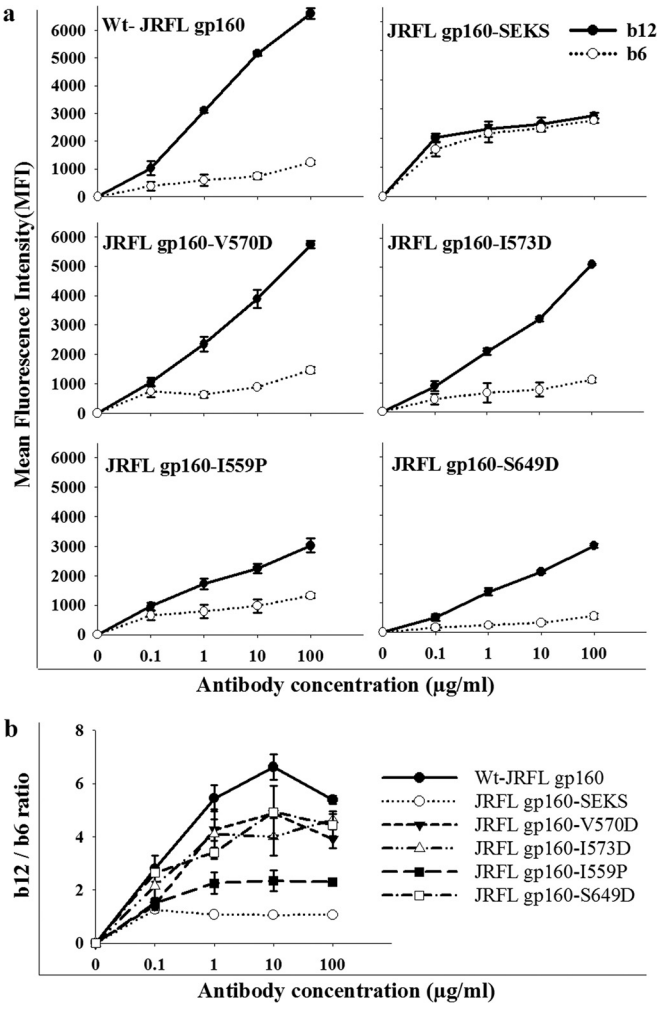

FIG 2 (a) Binding of gp120-directed CD4bs neutralizing (b12) and nonneutralizing (b6) antibodies to cleavage-competent JRFL Env, uncleaved JRFL Env, and JRFL Env with 6-HBD mutations. Proteins were expressed on the surfaces of HEK 293T cells. Antibody binding was characterized by FACS. MFIs were plotted against antibody concentrations. The experiment was repeated three times with similar results. wt gp160 and the gp160-V570D mutants showed the best discrimination between b12 and b6. gp160-SEKS is a cleavage site-defective mutant that shows no discrimination, in agreement with earlier results (16, 32). The symbols represent the mean values, and the error bars represent standard deviations derived from two independent experiments. Cell surface expression was carried out in HEK 293T cells. (b) b12 and b6 antibody binding MFI ratios were plotted as a function of the antibody concentration to analyze the conformational integrity of the CD4bs. The gp160-V570D, gp160-I573D, and gp160-S649D mutants showed patterns similar to that of wt gp160, whereas gp160-I559P and gp160-SEKS showed a significantly lower b12/b6 ratio. ($P < 0.05$; two-tailed unpaired t test at an antibody concentration of 10 μg/ml).

gp160 allowed high binding of b12, but not b6. The cell lysates from gp160-I559P-expressing cells showed approximately equal fractions of unprocessed gp160 and gp120, suggesting that incomplete cleavage of gp160-I559P contributes to the lower b12/b6 ratio observed for the mutant (Fig. 2). In contrast, gp160-V570D cell lysates showed efficient cleavage of gp160, similar to wt gp160.

In addition to gp120-specific antibodies, gp41-specific antibodies were also used to probe the integrity of Env in the presence of 6-HBD mutations. At lower concentrations of the gp41-specific antibodies 2F5 and 4E10, binding was low, as previously reported (see Fig. S3 in the supplemental material). The 2G12 and b12 neutralizing antibodies bound even at 0.01 μg/ml, but the 2F5 and 4E10 neutralizing antibody binding signals were prominent only at 1 μg/ml. This is expected, as the 2F5 and 4E10 epitopes are partially exposed and also neutralize HIV-1 only at higher concentrations (32). All 6-HBD mutants show similar binding to 2F5 and 4E10 antibodies. The 6-HBD mutants were also probed with the gp41-specific nonneutralizing antibody D49. This antibody bound weakly to wild-type and 6-HBD mutant Envs but showed significant binding to cleavage-defective Env (see Fig. S2 in the supplemental material). This indicates that the introduction of 6-HBD mutations retained the conformation of 2F5, 4E10, and D49 epitopes, similar to wild-type native Env. Cleavage-defective Env (gp160-SEKS) showed significantly higher binding to 2F5 than cleavage-competent Env (wt gp160), which is consistent with previous reports (32) (see Fig. S3 in the supplemental material).

To further probe the antigenic nature of gp120 trimers in Env and to monitor the accessibility of nonneutralizing epitopes on Env in the presence of 6-HBD mutations, cells were probed with anti-gp120 polyclonal sera. Since the anti-gp120 polyclonal sera were raised by immunization with monomeric JRCSF gp120, they are composed largely of nonneutralizing antibodies. Env-expressing cells were probed with various dilutions of anti-gp120 polyclonal sera. Cleavage-defective Env (gp160-SEKS)-expressing cells bound the polyclonal sera with higher affinity than cleavage-competent Env (wt gp160) and other 6-HBD mutants of Env (see Fig. S3 in the supplemental material). Surprisingly, the gp160-I559P mutant also showed slightly higher binding to polyclonal sera, whereas gp160-V570D-, gp160-I573D-, and gp160-S49D-expressing cells showed binding to polyclonal sera similar to that of wt-gp160-expressing cells (see Fig. S3 in the supplemental material). Within the limited resolution of the above-described experiments, the V570D, I573D, and S649D mutations thus did not affect the native conformation of Env and showed negligible exposure of nonneutralizing epitopes.

Our data suggest that 6-HBD mutations did not substantially perturb the native conformation of gp41 trimers, which in turn led to retention of a native-like gp120 trimer conformation in Env. Though it destabilized six-helix bundle formation efficiently, I559P appeared to perturb the native Env conformation on the cell surface. Of the various 6-HBD mutations examined, the V570D and I573D mutations caused the least perturbation of the native Env trimers on the cell surface and did not bind to various Env-directed nonneutralizing antibodies.

6-HBD mutations diminish shedding of gp120 from Env. In the virus entry process, six-helix bundle formation occurs after CD4-induced conformational changes (Fig. 4a) (1, 4, 40). In the fusion process, gp120 is believed to be shed from the Env surface once Env attains the pre-hairpin intermediate conformation (Fig. 4a). It has been previously suggested that destabilization of structures involved in fusion may stabilize Env in a native-like conformation (25, 39, 41). Such mutations could either abolish the formation of both the pre-hairpin intermediate and the 6-HB (mutations that disrupt the NHR trimer) or the 6-HB alone (mutations that disrupt NHR and CHR interactions). One way to probe Env stabilization is by quantitating sCD4-induced gp120 shedding. We therefore examined whether the 6-HBD mutations characterized above stabilize native Env by quantitating sCD4-induced shed gp120 levels from Env expressed on the cell surface.

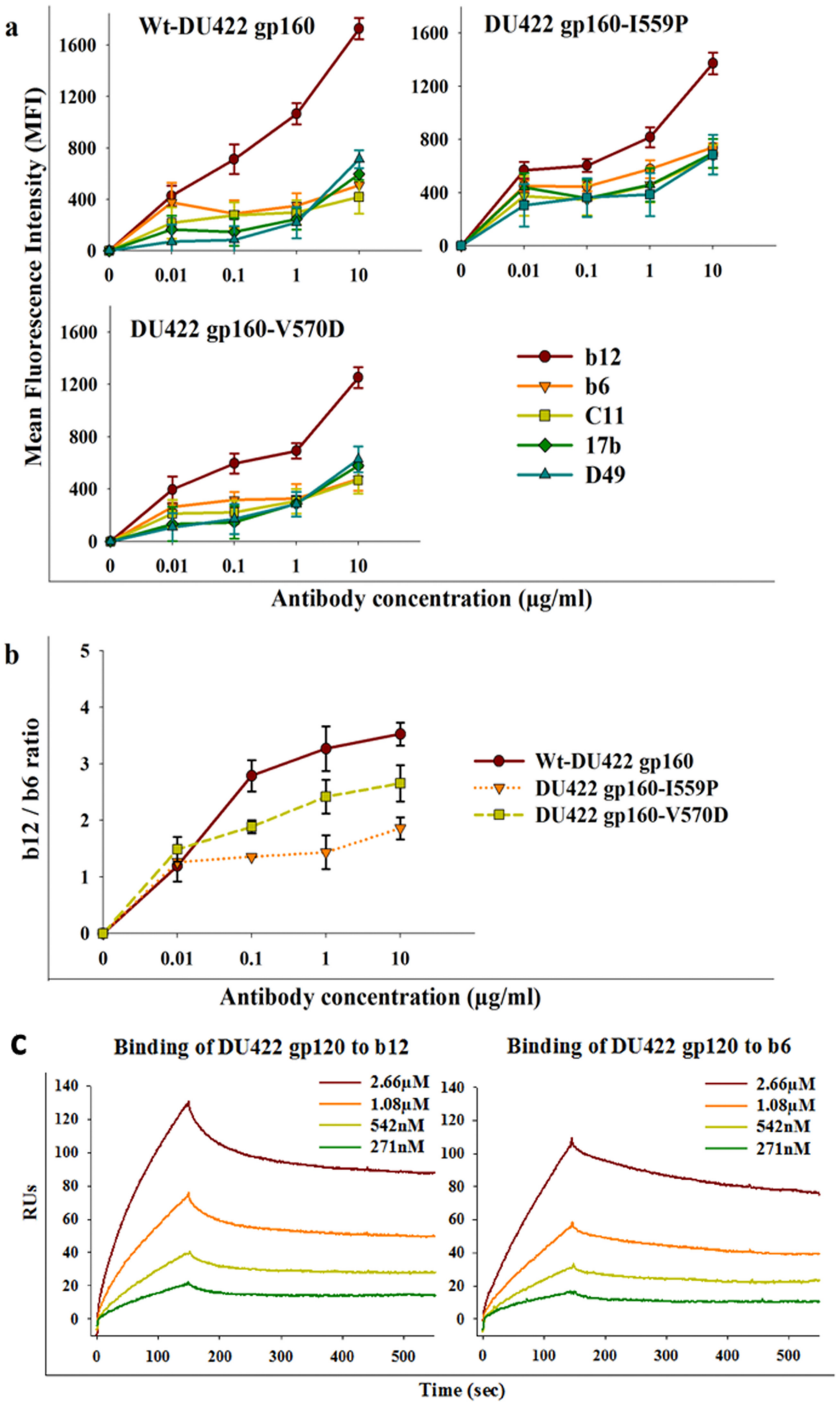

FIG 3 (a) Binding of neutralizing (b12) and nonneutralizing (b6, C11, 17b, and D49) antibodies to Env from a subtype C isolate (DU422) with I559P and V570D mutations. DU422 Env constructs were expressed on the HEK 293T cell surface and probed with different antibodies. Binding of antibodies was characterized by FACS. Binding MFIs are shown as a function of the antibody concentration. The symbols represent the mean values, and the error bars represent the standard deviations derived from two independent experiments. (b) MFI ratios of b12 and b6 antibody binding were plotted as a function of the antibody concentration to compare the CD4bs integrity of 6-HBD mutants of DU422 Env. (c) SPR studies to confirm that monomeric DU422 gp120 retains the epitopes for b12 and b6 antibodies. Shown are sensogram overlays for binding of different concentrations of monomeric DU422 gp120 to surface-immobilized b12 (left) and b6 (right) antibodies. The response units are plotted as a function of time. The K_D (equilibrium dissociation constant) values for b12 and b6 are 240 ± 20 nM and 340 ± 17 nM, respectively.

To detect shed gp120 levels, we used FACS and ELISA methodologies. For ELISA, HEK 293T cells were transfected with either wt gp160 or gp160 with 6-HBD mutations. Forty-eight hours posttransfection, cells were harvested and incubated with sCD4 for 2 h. It has been reported that sCD4 induces conformational changes in gp120, which leads to shedding of gp120, followed by six-helix bundle formation (8, 42). Shed gp120 levels in supernatants were measured by ELISA. Shed gp120 in supernatants was

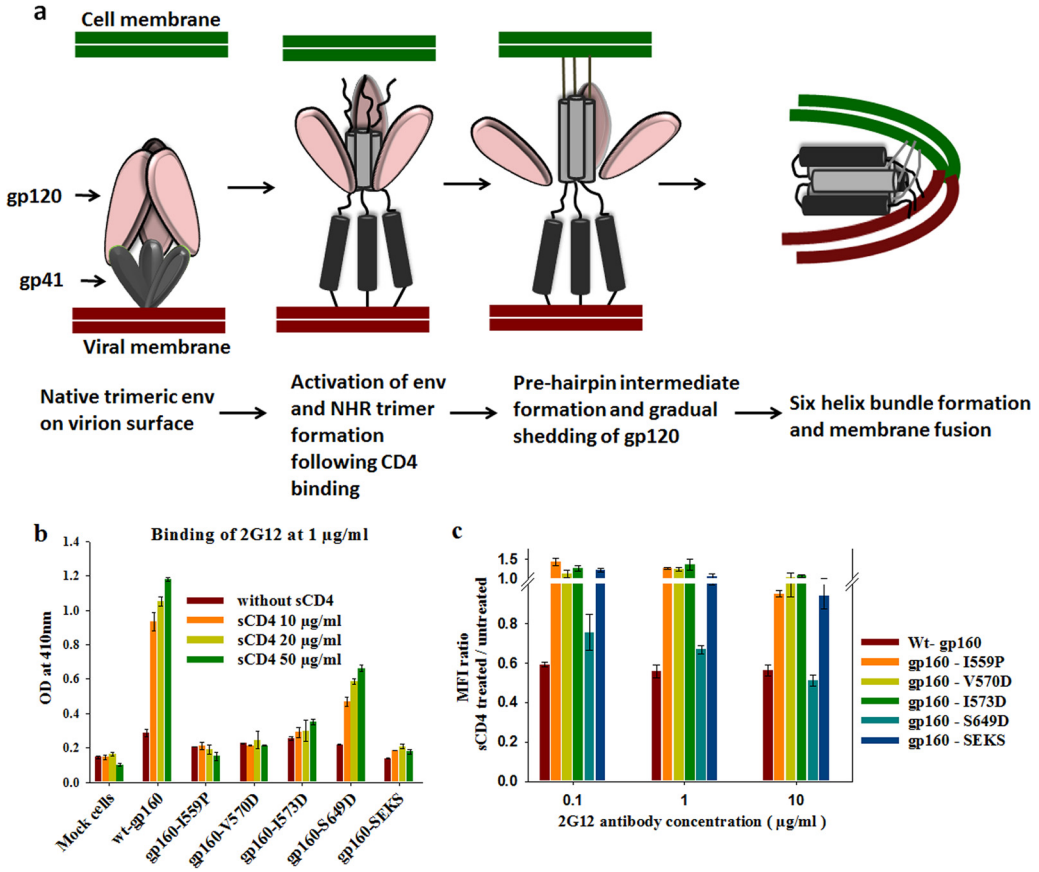

FIG 4 (a) Cartoon representation of fusion based on the current understanding of the HIV-1 Env trimer-mediated fusion process. (b) 6-HBD mutants abolish sCD4-induced shedding of gp120 from Env expressed on the cell surface, as determined by ELISA. Env-expressing cells were incubated with sCD4 to allow gp120 shedding from Env on the cell surface. The shed gp120 in the supernatant was collected and captured on ELISA plate wells by gp120-capturing antibody (D7324). The amount of shed gp120 was quantitated by 2G12 antibody binding. OD, optical density. The error bars indicate the standard deviations obtained from three independent experiments. (c) 6-HBD mutants abolish sCD4-induced shedding of gp120, as determined by FACS. 6-HBD mutant proteins were expressed on the cell surface. Cells were incubated with sCD4 to induce gp120 shedding. The shed gp120 from the cell surface was washed off, and the gp120 on the cell surface was quantitated by staining the cells with 2G12 antibody. The ratio of MFIs from sCD4-treated and untreated cells was plotted as a function of the 2G12 antibody concentration. The error bars indicate standard deviations obtained from two independent experiments.

captured by a gp120 capture antibody (D7324), with which ELISA plate wells were coated, and detected by probing with 2G12 antibody. wt gp160-transfected cells shed gp120 upon sCD4 incubation. Introduction of 6-HBD mutations (particularly I559P, V570D, and I573D) greatly diminished gp120 shedding from Env (Fig. 4b). I559P and V570D mutants showed complete absence of gp120 shedding from the cell surface. The gp160-S649D mutation did not decrease shedding, possibly because it either failed to sufficiently destabilize the six-helix bundle or because it altered the gp41 native conformation, which in turn disrupts gp120-gp41 interaction (Fig. 4b).

In the FACS-based method, 48 h after transfection, cells were harvested and incubated with sCD4 (50 μg/ml) for 2 h. After washing the cells to remove shed gp120, the cells were probed with 2G12 antibody to probe the amount of gp120 retained on the cell surface. The results from FACS correlated well with those from ELISA (Fig. 4c). Only wt JRFL gp160- and JRFL gp160-S649D-transfected cells shed gp120 upon sCD4 incubation. Other 6-HBD mutants greatly abolished shedding of gp120 when incubated with sCD4 and also showed a slight increase in binding to 2G12 neutralizing antibody in the presence of sCD4 (Fig. 4c).

We have also assessed the binding of cell surface-expressed 6-HBD Env mutants to D49 monoclonal antibody, an antibody specific for the cluster I (immunodominant) region in gp41, which is inaccessible on the native Env trimer (43, 44). The cluster I region is occluded on Env due to gp41 and gp120 interaction. When gp120 is shed from the cell surface, the cluster I region from gp41 becomes accessible. The binding of D49 antibody is directly proportional to the shedding of gp120. Forty-eight hours after transfection, cells were harvested and incubated with sCD4 for 2 h. After washing the cells to remove shed gp120, the cells were probed with D49 antibody. As expected, D49 antibody binding to wt gp160-expressing cells increased significantly (~4-fold) after sCD4 incubation (Fig. 5). Cleavage-defective Env (gp160-SKES) and the S649D mutant also showed increased binding to D49 in the presence of sCD4. I559P, V570D, and I573D mutants did not show any change in D49 binding with and without sCD4. Cleavage-defective Env (gp160-SEKS) did not allow gp120 shedding because of covalent linkage between gp120 and gp41 (Fig. 4b and c). It bound surprisingly well to D49 antibody in the presence of sCD4 (Fig. 5). This indicates that the cluster I region shows increased accessibility upon CD4 binding in cleavage-defective Env,

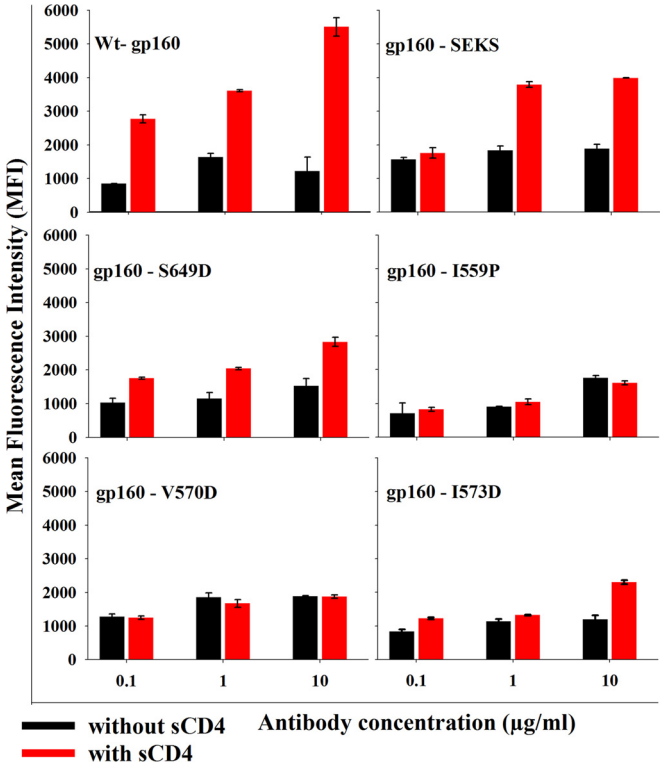

FIG 5 6-HBD mutations prevent sCD4-induced shedding of gp120 and diminish the accessibility of the gp41 cluster I epitope while retaining gp120-gp41 interactions. The gp41 cluster I region is an immunodominant region that is occluded due to gp120-gp41 interactions in native trimers. Shedding of gp120 results in an increase in the accessibility of the cluster I region recognized by the monoclonal antibody D49. To examine the ability of 6-HBD mutations to abolish gp120 shedding and to retain gp120-gp41 interactions, Env-expressing cells were stained with D49 antibody after sCD4-induced gp120 shedding from the cell surface. MFIs are plotted as a function of the D49 antibody concentration. The error bars indicate the standard deviations obtained from two independent experiments.

even though gp41 and gp120 are covalently linked. sCD4-induced gp120 shedding experiments suggested that 6-HBD mutations prevented shedding of gp120 by stabilizing a native-like Env conformation. I559P and I573D are located at the "a" positions of the NHR. These mutations destabilize the core NHR trimer essential for pre-hairpin intermediate formation and 6-HB formation and abolish gp120 shedding. In contrast, the V570D mutation is located at the "e" position in the NHR region; it is expected to destabilize 6-HB formation by preventing NHR and CHR interactions and should show little effect on the pre-hairpin intermediate. Surprisingly, shed gp120 experiments showed that the V570D mutation, apart from destabilizing 6-HB formation, also abolished gp120 shedding.

Disulfide bond-stabilized cell surface JRFL Env trimers deviate from the native Env trimer conformation. Previous studies have attempted to stabilize interactions between gp120 and gp41 in the Env trimer by engineering disulfide bonds between residue 501 of gp120 and 605 of JRFL gp41 (27, 39) ectodomains. This disulfide-bonded mutant is referred to as SOS-gp140. SOS-gp140 was reported to be cleaved efficiently when expressed and was predominantly monomeric. Further, the I559P mutation was introduced into SOS-gp140 to give SOSIP-gp140. SOSIP-gp140 was predominantly trimeric and cleaved. When immunization studies were done with trimeric SOSIP-gp140, it elicited a marginally improved antibody response compared to monomeric gp120-immunized animals (30, 45). The sera neutralized tier 1 viruses with high titers and some tier 2 viruses with low titers. The cryo-EM structure of SOSIP-gp140 was solved and compared with that of native Env trimers (19, 40, 46). The cryo-EM and crystal structures suggest that SOSIP-gp140 showed topology similar to that of native Env trimers (46). Hence, we made SOS and SOSIP mutants in a JRFL gp160 background, expressed them on the cell surface, and probed their conformations with various antibodies.

Introduction of the SOS mutation in JRFLgp160 led to lower levels of expression of Env on the cell surface, as probed by 2G12 binding. This might be due to reduced incorporation of Env in the membrane due to mutations or formation of nonnative conformations. Binding MFI values were normalized for expression levels based on 2G12 antibody binding. We observed that the b12 and b6 binding difference was small in SOSIP-gp160 compared to wt gp160 trimers on the cell surface (Fig. 6a). This could be because the engineered disulfide perturbed the native Env conformation or could be due to inefficient cleavage of envelope after its synthesis. We also tested the V570D mutation, which is a promising 6-HBD mutation, in the context of SOS-gp160 (SOS gp160-V570D). SOS-gp160-V570D exhibited a pattern of binding to CD4bs neutralizing and nonneutralizing antibodies similar to that of SOSIP-gp160 (Fig. 6a). To further investigate this, we transfected a plasmid encoding furin along with the disulfide constructs to allow improved cleavage of envelope mutants, but it did not help (Fig. 6a). To further improve cleavage, we introduced six arginine residues (R6) in place of the REKR cleavage sequence (a technique that was used previously to enhance the cleavage of SOS-gp140 [30]), which resulted in increased expression (Fig. 6a). SOS-gp160 showed ~2.5-fold difference in b12 and b6 binding, which is better than the SOSIP-gp160 binding pattern (Fig. 6b). Hence, the disulfide bond engineered to lock gp120 and gp41 appears to have perturbed the native conformation of Env, though the soluble-disulfide-stabilized gp140 constructs were previously shown to be trimeric and cleaved efficiently (26, 29). As cleavage levels of Env correlate with the antibody binding profiles, it is important to know the degree of cleavage of disulfide-stabilized Env mutants. The cleavage of disulfide-stabilized Env trimers was probed using Western blotting. Equal amounts of total cell lysates of Env-expressing cells were subjected to SDS gel electrophoresis, transferred to a nitrocellulose membrane, and probed with rabbit anti-gp120 polyclonal sera (Fig. 6c). The cell lysates from wt-gp160-transfected cells showed the presence of efficiently cleaved Env (presence of gp120), though a small amount of residual unprocessed and hyperglycosylated gp160 was detected, as seen previously (16) (Fig. 6c). Similar to wt gp160, the disulfide bond-engineered Envs (gp160-SOSIP, gp160-SOS-V570D, and gp160-SOS) showed efficient cleavage of gp160 with a small amount of unprocessed gp160, though the level of expression was lower than that of wt gp160 in all cases (Fig. 6c). Furin overexpression further increased the cleavage of disulfide mutant Env mutants (Fig. 6c). Cleavage-defective Env cell lysates were used as a control to indicate the positions of unprocessed gp160. These results confirm that the disulfide mutant Envs are properly cleaved and that the lower b12/b6 binding ratios relative to the wild type in the SOS mutants are due to altered Env conformation rather than decreased cleavage.

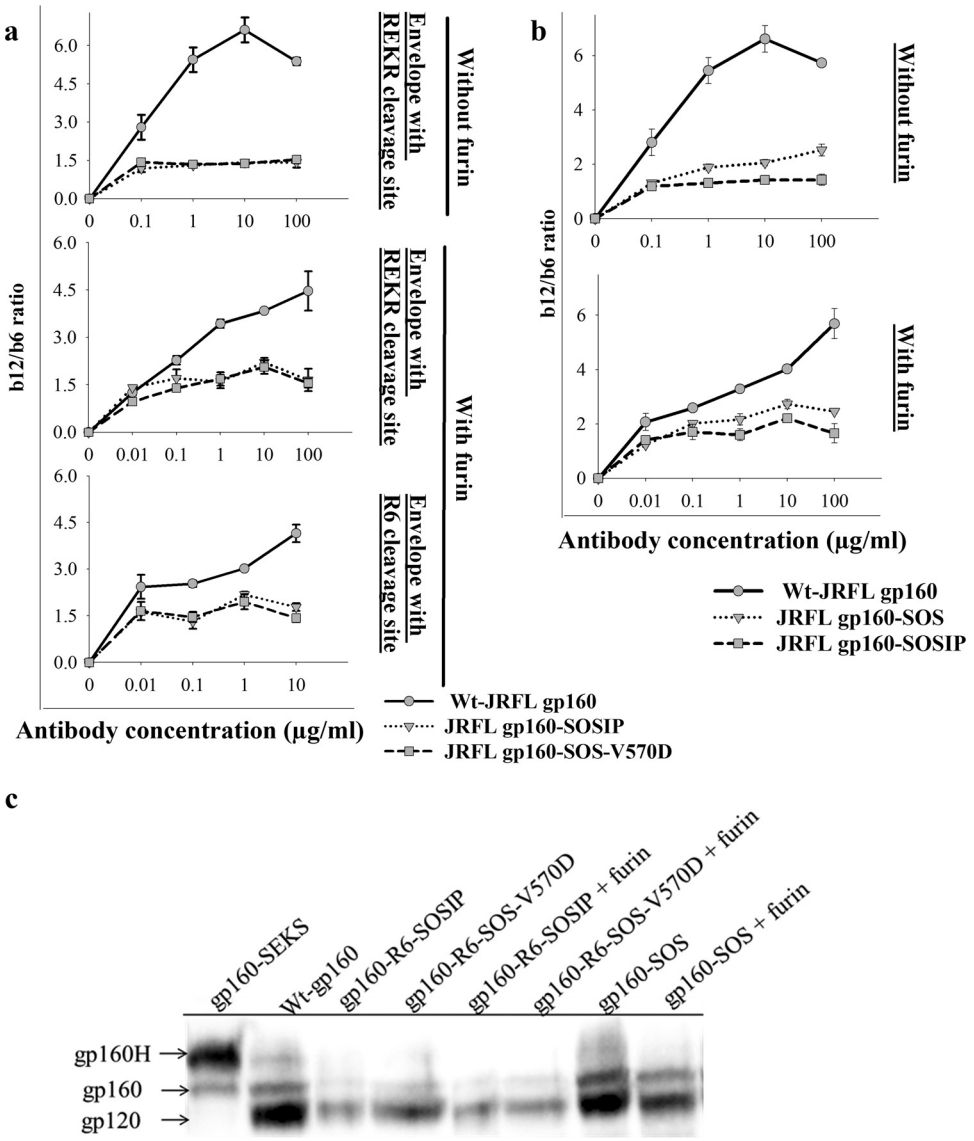

FIG 6 Engineered disulfide bonds between gp120 and gp41 perturb the native conformation of JRFL Env. Disulfide bond (SOS) mutants of Env were expressed on the HEK 293T cell surface. (a) Disulfide bond Env mutants with I559P and V570D mutations. To probe for conformational similarity to native Env, cells were stained with CD4bs neutralizing (b12) and nonneutralizing (b6) antibodies. Antibody binding was characterized by FACS. The ratios of b12 and b6 antibody binding MFIs are plotted as a function of the antibody concentration. In the context of SOS, both the V570D and I559P mutations show a lower b12/b6 ratio than the wt without SOS. (b) Wt Env with the SOS disulfide was only marginally more native-like than disulfide-stabilized Env with 6-HBD mutations. The binding studies were done as described for panel a. Introduction of the SOS disulfide bond between residues A501C and T605C thus results in substantially decreased discrimination between b12 and b6 antibodies. (c) Cleavage of disulfide-stabilized Envs analyzed by Western blotting. Equal volumes of total cell lysates from Env-transfected cells were transferred to nitrocellulose membranes and probed with rabbit anti-gp120 polyclonal sera. gp160H is a higher-molecular-weight hyperglycosylated species described in previous studies (16). gp160-SOSIP and gp160-SOS-V570D are both largely cleaved but are expressed at lower levels than wt gp160 or SOS-gp160. Coexpression of furin marginally increased the extent of cleavage for these mutants but had less effect on cleavage of SOS-gp160.

We have also examined the binding of gp41 MPER antibodies to SOS-gp160 mutants. The 2F5 and 4E10 epitopes are partially accessible to these antibodies in native Env and are exposed during the fusion process, particularly in the pre-hairpin intermediate stage (4, 47–49). Consequently, the 2F5 and 4E10 antibodies neutralize HIV-1 only at high concentrations, and a recent study has shown that these antibodies required prolonged incubation times to completely inactivate the virus (50). We examined the binding of 2F5 and 4E10 antibodies to SOS-gp160 mutants. Both gp160-SOSIP and SOSgp160-V570D bound better to 2F5 (~4-fold) and 4E10 (~3-fold) antibodies than wt gp160 (Fig. 7). Transfection of disulfide Env mutants with furin or replacement of REKR with an R6 cleavage site did not result in any significant change (Fig. 7). The high binding of 2F5 and 4E10 antibodies to disulfide mutants suggests increased accessibility of the MPER region in gp41, consistent with a perturbed trimer conformation. The MPER region is occluded in the native trimeric Env complex. A recent study showed that the 2F5 epitope is accessible on laboratory-adapted sensitive viruses, but not on neutralization-resistant viruses, such as JRFL (49). Thus, these results indicate that disulfide engineer-

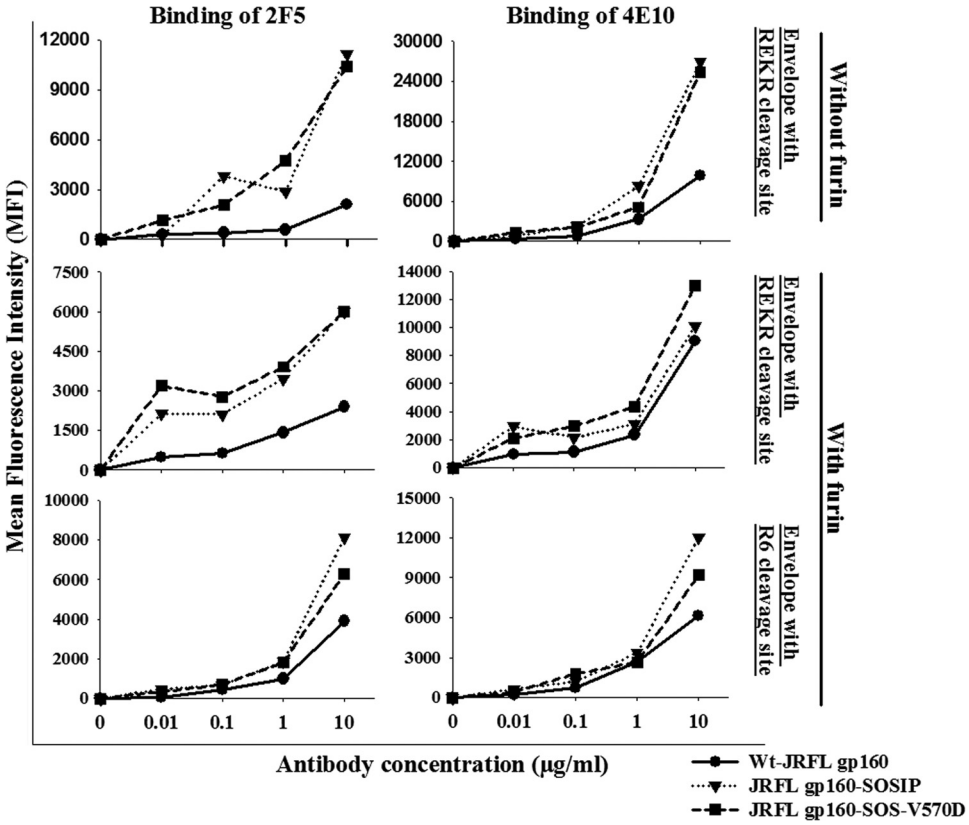

FIG 7 Introduction of a disulfide bond between JRFL gp120 and gp41 results in increased exposure of the 2F5 and 4E10 epitopes. Env-expressing cells were probed with the gp41-directed antibodies 2F5 and 4E10. MFIs were normalized for cell surface expression based on 2G12 antibody binding. The native conformation of gp41 was perturbed in Env disulfide mutants, and coexpression of furin enabled the Env disulfide mutants to form a more native-like gp41 MPER epitope. Two independent transfection experiments were performed with similar results.

ing in JRFL Env resulted in structural reorganization with enhanced exposure of gp41 epitopes, which are occluded in native Env. The cysteine mutation introduced in gp41 is proximal to the native disulfide in gp41. We cannot exclude the possibility that the extra cysteine could form a nonphysiological disulfide bond with cysteine present in gp41 in the cell surface expression system used here.

PG9 and PG16 are quaternary, epitope-specific, broadly neutralizing antibodies. These antibodies recognize variable loop region epitopes on gp120 in the context of the trimer (17, 51). Since wt JRFL gp160 does not bind to PG9 and PG16, we introduced the E168K mutation to detect PG9 and PG16 binding (17). The E168K mutation was introduced into wt JRFL gp160, JRFL gp160-V570D, SOSIP-gp160, and SOS-gp160-V570D backgrounds for PG9 and PG16 antibody binding studies. Binding of PG9 and PG16 antibodies was significantly less to SOSIP-gp160-E168K than to wt JRFL gp160-E168K, but the coexpression of furin slightly improved binding to PG9 and PG16 (Fig. 8a). SOSIP-gp160-E168K and SOSgp160-V570D mutants bound ~5-fold and ~2-fold more weakly to PG9 and PG16 on the cell surface than wt gp160-E168K (Fig. 8a). Replacing the cleavage site (REKR) with R6 improved the binding of PG9 and PG16 antibodies. The gp160-E168K and gp160-V570D-E168K mutants exhibited similar binding to PG9 and PG16 (Fig. 8b).

DISCUSSION

In this study, we have characterized postfusion six-helix bundle-disrupting mutations in the context of native Env trimers on the cell surface. Native trimeric HIV-1 Env exists in a metastable conformation that is prone to form the highly stable postfusion six-helix bundle conformation (4, 40). Mutations that interrupt coiled-coil packing will destabilize the pre-hairpin intermediate state and/or postfusion six-helix bundle formation and allow the Env trimer to lock into the native conformation, where nonneutralizing epitopes are expected to be occluded and neutralizing epitopes are exposed efficiently. After CD4 receptor binding, Env attains a more open quaternary-state conformation (52), and it exposes immunodominant epitopes that are occluded on native trimeric Env. In our previous work, we have screened various mutations in NHR and CHR repeat regions (I559P, V570D, I573D, and S649D) that disrupt six-helix bundle formation on the yeast surface (31). We introduced these mutations into Env trimers and expressed them on the mammalian cell surface to characterize the mutations in the context of the native Env trimer. Binding studies with various gp120- and gp41-specific antibodies showed that the six-helix bundle-destabilizing mutations (particularly V570D and I573D) did not perturb the native trimer conformation.

It was previously shown that the I559P mutation, in combination with the A501C and T605C mutations, stabilizes a trimeric,

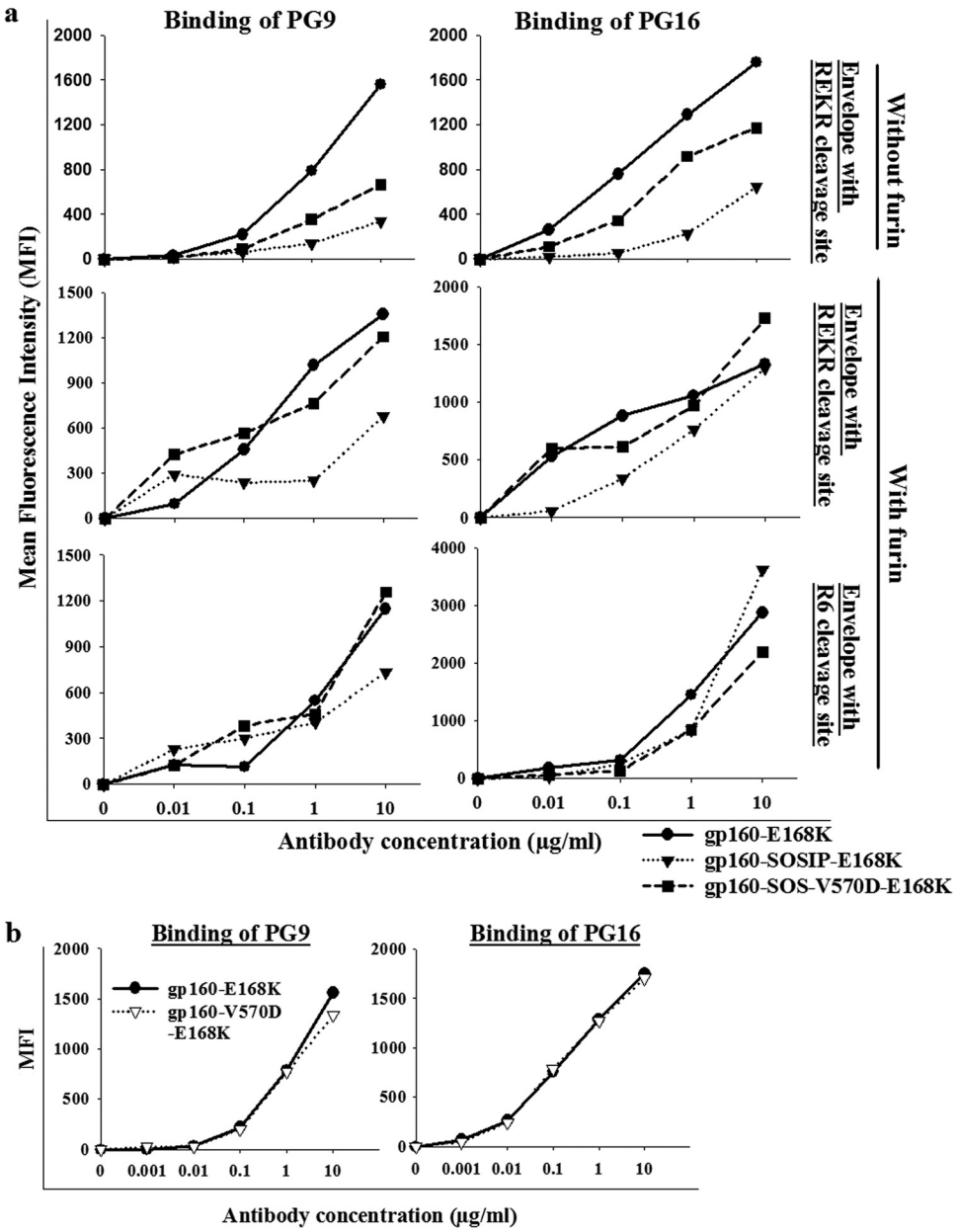

FIG 8 SOS mutations decrease binding to gp120 trimer-specific antibodies PG9 and PG16, but binding was increased in the presence of the R6 cleavage site and with furin coexpression. (a) Cells expressing disulfide Env mutants were stained with quaternary specific antibodies PG9 and PG16. Cell surface expression levels were detected by 2G12 antibody binding. (b) Cells expressing wt gp160 and gp160-V570D without the SOS mutation were stained with PG9 and PG16. The two envelopes showed identical binding. The MFIs were normalized for cell surface expression based on 2G12 antibody binding. Two independent transfection experiments yielded similar results.

native-like conformation of Env (28, 39). Residue 559 occurs at the "a" position of the NHR, and mutations at this position disrupt or destabilize the NHR homotrimer present in the pre-hairpin intermediate and the postfusion 6-HB. The conformation of the entire NHR region in native Env is not definitively known, though a substantial part of it is helical and homotrimeric (19–21). If residue 559 remains at the "a" position of the NHR homotrimer in native Env, then it is possible that the I559P mutation may distort or destabilize the native Env structure, in addition to its destabilizing effect on the 6-HB. Even if this region is not helical in native Env, introduction of proline could perturb the structure, given its constrained main chain dihedral angle Φ value of approximately −65° and lack of an amide hydrogen (53). Since the NHR-CHR interface is not formed in native Env (19–21), it is important to explore the effects of mutations in this interface region on the stability of native Env. The present study shows that I559P appears to perturb the native conformation of JRFL Env more than V570D, though both destabilize the postfusion conformation. Shed gp120 experiments suggest that six-helix bundle-destabilizing mutations were able to lock Env in a native-like conformation while destabilizing the postfusion six-helix bundle. Mutations in both the NHR and CHR regions of gp41 did not

affect the ability of gp120 subunits to bind neutralizing and nonneutralizing antibodies, and additionally, they prevented sCD4-induced gp120 shedding from the cell surface by shifting the equilibrium toward the native conformation. The results suggest that wild-type cleaved Env in the native trimer, once bound to CD4, is able to transiently access conformations in which gp41 can form a six-helix bundle or, minimally, conformations in which regions of NHR and CHR interact as they do in the 6-HB.

Stabilizing Env in its native conformation is an important problem in HIV-1 vaccine design. The labile nature of native Env coupled with the high stability of coiled coils formed by NHR and CHR of gp41 (4) means that native Env exists in a metastable conformation. Structural changes in gp41 regions are linked with conformational changes in gp120. The six-helix bundle-destabilizing mutations screened in this study did not alter the native conformation of gp120 trimer on Env (Fig. 2). We show that postfusion 6-HBD mutations help retain gp120 on the cell surface, in part by preventing the sCD4-induced gp120 shedding process that occurs prior to fusion (Fig. 4 and 5). 6-HBD mutations did not alter the quaternary conformation of Env, which was probed by PG9 and PG16 antibodies. The quaternary conformational epitopes at the apex of the gp120 trimer (V1/V2 regions) are stable due to the existence of gp41 in a native-like conformation. The 6-HBD mutations tested here diminished misfolding of Env and assisted the display of native-like Env on the cell surface. In an alternative approach, Crooks et al. (54) described enzymatic strategies to remove nonnative forms of Env (junk Env) from virus-like particles. The current 6-HBD mutations provide a genetic strategy to minimize misfolding of Env on the cell surface.

Among the 6-HBD mutations characterized in this study, the I559P and I573D mutations are at the hydrophobic core of the postfusion NHR trimer and the V570D and S649D mutations are at the corresponding NHR-CHR interface. The I559P mutation prevented gp120 shedding but partially exposed nonneutralizing epitopes, as well. This suggests that in the context of the JRFL sequence, the I559P mutation might have caused subtle changes in the native gp41 conformation that alter cleavage efficiency and gp120 conformation in Env trimers. In contrast, V570D and I573D mutations did not appear to perturb the native trimer integrity as assessed by antibody binding to CD4bs (b12 and b6), CD4-induced epitopes (17b), V1/V2 quaternary epitopes (PG9 and PG16), and gp41 cluster I (D49) and MPER (2F5 and 4E10) epitopes. The V570D, I573D, and I559P mutations all abolished gp120 shedding in the presence of sCD4 and have slightly increased binding of 2G12 neutralizing antibody in the presence of sCD4. Although the S649D mutation disrupted six-helix bundle formation on the yeast surface and maintained trimer integrity (31), it failed to abolish gp120 shedding from the Env trimer in the presence of sCD4. gp160-SEKS is a cleavage-defective Env in which the cleavage site between gp120 and gp41 is mutated to covalently link gp120 and gp41. Immunization studies with cleavage-defective Env have failed to elicit neutralizing antibodies. Cleavage-defective Env bound equally well to both neutralizing (b12) and nonneutralizing (b6) antibodies (16). The deviation from the native Env conformation and exposure of nonneutralizing epitopes are further confirmed by its increased binding to anti-gp120 polyclonal sera and other nonneutralizing monoclonal antibodies. Due to the presence of covalent linkage between gp120 and gp41 at the cleavage site, cleavage-defective Env prevented sCD4-induced gp120 shedding but exposed immunodominant regions (the cluster I region) of gp41 in the presence of sCD4. The MPER region, which is partially buried in the native Env conformation, was exposed in cleavage-defective Env (32). Cleavage-defective Env failed to stabilize Env in the native conformation and instead presented nonneutralizing epitopes, which likely dominate the immune response.

In previous studies, gp120 and gp41 interactions were stabilized by introducing a disulfide bond between the gp120 and gp41 subunits, along with the I559P mutation. gp140 constructs with these three mutations are referred to as SOSIP-gp140 (27, 39). SOSIP-gp140 was cleaved efficiently following cotransfection with furin and formed a significant amount of trimeric species. Immunization studies showed that soluble, disulfide-stabilized SOSIP-gp140 immunogens are better at eliciting neutralizing antibodies than monomeric gp120 immunogens (30). Although they have failed to elicit neutralizing antibodies that can neutralize diverse HIV-1 isolates, they are among the better trimeric Env immunogens designed so far. Cryo-EM structural analysis of SOSIP-gp140 trimers indicated that their topology is similar to that of native HIV-1 Env trimers (46). In native Env trimers, three gp120 molecules associate at the apex of the envelope to form quaternary epitopes that are targets for cross protective neutralization (19, 20, 52). PG9 and PG16 antibodies are quaternary specific antibodies, and they recognize the V1/V2 regions of gp120 in the native trimer conformation. Soluble KNH1144 SOSIP-gp140 trimers were poorly recognized by PG9 and PG16 antibodies in ELISA studies in earlier reports (17), though significant binding was recently seen with BG505 SOSIP-gp140 (28). In the present study, we have shown that JRFL SOSIP Env trimers on the cell surface deviated from the native Env conformation and bound weakly to the quaternary specific PG9 and PG16 antibodies. Introduction of the V570D mutation instead of the I559P mutation in SOSIP-gp160 increased binding to PG9 and PG16. On the cell surface, disulfide bond-stabilized trimers without the I559P mutation (SOS-gp160) are better mimics of native conformation than SOSIP-Env trimers (SOSIP-gp160) (Fig. 6), but soluble SOS-gp140 immunogens are predominantly monomeric when expressed and purified in soluble form (26, 39). The cryo-EM structures of the SOS-gp160ΔCT trimer exhibited a tripod conformation (55), although the native Env trimer does not exist in a tripod conformation (40, 52). The cryo-EM structures of soluble KNH1144 and JRFL SOSIP-gp140 trimers were also solved (46, 56). In these structures, the densities at the gp120 trimer association interface where quaternary neutralizing epitopes exist are weak compared to those of native HIV-1 Env trimers. This might be due to the lack of proper gp120 trimer association at the apex of the Env trimer. Our studies with quaternary specific PG9 and PG16 antibodies are consistent with the weak gp120 trimer association densities in these disulfide trimers (Fig. 8). However, recent studies of SOSIP gp140 derivatives from the BG505 isolate with MPER deleted have indicated that these derivatives are quite similar to native Env in terms of antibody binding profiles (28). It would therefore be interesting to compare the V570D, I573D, and I559P mutants in this background. The difference in stability of Env on the cell surface and in soluble form makes it difficult to directly compare 6-HBD mutations on the cell surface and in soluble constructs. The TM domain in cell surface Env may make an additional contribution to stability relative to soluble constructs, which lack TM and in some cases the MPER region. Since, BG505 trimers with TM and MPER de-

leted are stable, the 6-HBD mutations described here can also be incorporated into such soluble constructs.

An ideal HIV-1 trimeric Env immunogen should expose neutralizing epitopes and occlude immunodominant nonneutralizing epitopes. Stabilization of Env in its native conformation will assist in the design of improved vaccine candidates that may elicit cross protective neutralizing antibodies. The mutations reported here (V570D and I573D) destabilize the postfusion conformation while minimally perturbing the native conformation, indicating these residues are surface proximal in native Env. Residue 573 is at the a position of the NHR. However, the present data indicate that this region, which is located close to the C terminus of the NHR in the 6-HB, is unlikely to be part of a homotrimeric coiled coil in native Env, since burial of aspartic acid at the interior of the homotrimer is expected to be highly destabilizing (37, 57). It was recently reported (58) that DNA priming with JRFL Env and tat followed by a gp140 protein boost elicited encouraging neutralization in nonhuman primates. The V570D and I573D mutations described above can also be used to stabilize native Env in a DNA vaccine format.

ACKNOWLEDGMENTS

We thank J. P. Moore for the furin expression plasmid, pCDNA furin; R. Wyatt for pSVIII-JRFL g160 and pctat plasmids; and the Neutralizing Antibody Consortium and the NIH AIDS Research and Reference Program for various HIV-1-directed monoclonal antibodies.

This work was funded by grants from the International AIDS Vaccine Initiative and the Departments of Biotechnology and Science and Technology, Government of India, to R.V. Sannula Kesavardhana is the recipient of a fellowship from the Council of Scientific and Industrial Research, Government of India. We thank V. Vamsee Aditya Mallajosyula and Ujjwal Rathore for helpful discussions.

REFERENCES

1. **Wyatt R, Sodroski J.** 1998. The HIV-1 envelope glycoproteins: fusogens, antigens, and immunogens. Science **280:**1884–1888. http://dx.doi.org/10.1126/science.280.5371.1884.
2. **Center RJ, Leapman RD, Lebowitz J, Arthur LO, Earl PL, Moss B.** 2002. Oligomeric structure of the human immunodeficiency virus type 1 envelope protein on the virion surface. J. Virol. **76:**7863–7867. http://dx.doi.org/10.1128/JVI.76.15.7863-7867.2002.
3. **Wu L, Gerard NP, Wyatt R, Choe H, Parolin C, Ruffing N, Borsetti A, Cardoso AA, Desjardin E, Newman W, Gerard C, Sodroski J.** 1996. CD4-induced interaction of primary HIV-1 gp120 glycoproteins with the chemokine receptor CCR-5. Nature **384:**179–183. http://dx.doi.org/10.1038/384179a0.
4. **Chan DC, Fass D, Berger JM, Kim PS.** 1997. Core structure of gp41 from the HIV envelope glycoprotein. Cell **89:**263–273. http://dx.doi.org/10.1016/S0092-8674(00)80205-6.
5. **Weiss RA, Clapham PR, Cheingsong-Popov R, Dalgleish AG, Carne CA, Weller IV, Tedder RS.** 1985. Neutralization of human T-lymphotropic virus type III by sera of AIDS and AIDS-risk patients. Nature **316:**69–72. http://dx.doi.org/10.1038/316069a0.
6. **Moore JP, Sodroski J.** 1996. Antibody cross-competition analysis of the human immunodeficiency virus type 1 gp120 exterior envelope glycoprotein. J. Virol. **70:**1863–1872.
7. **Wyatt R, Desjardin E, Olshevsky U, Nixon C, Binley J, Olshevsky V, Sodroski J.** 1997. Analysis of the interaction of the human immunodeficiency virus type 1 gp120 envelope glycoprotein with the gp41 transmembrane glycoprotein. J. Virol. **71:**9722–9731.
8. **Kwong PD, Wyatt R, Robinson J, Sweet RW, Sodroski J, Hendrickson WA.** 1998. Structure of an HIV gp120 envelope glycoprotein in complex with the CD4 receptor and a neutralizing human antibody. Nature **393:**648–659. http://dx.doi.org/10.1038/31405.
9. **Kwong PD, Doyle ML, Casper DJ, Cicala C, Leavitt SA, Majeed S, Steenbeke TD, Venturi M, Chaiken I, Fung M, Katinger H, Parren PW, Robinson J, Van Ryk D, Wang L, Burton DR, Freire E, Wyatt R, Sodroski J, Hendrickson WA, Arthos J.** 2002. HIV-1 evades antibody-mediated neutralization through conformational masking of receptor-binding sites. Nature **420:**678–682. http://dx.doi.org/10.1038/nature01188.
10. **Kwon YD, Finzi A, Wu X, Dogo-Isonagie C, Lee LK, Moore LR, Schmidt SD, Stuckey J, Yang Y, Zhou T, Zhu J, Vicic DA, Debnath AK, Shapiro L, Bewley CA, Mascola JR, Sodroski JG, Kwong PD.** 2012. Unliganded HIV-1 gp120 core structures assume the CD4-bound conformation with regulation by quaternary interactions and variable loops. Proc. Natl. Acad. Sci. U. S. A. **109:**5663–5668. http://dx.doi.org/10.1073/pnas.1112391109.
11. **Schultz AM, Bradac JA.** 2001. The HIV vaccine pipeline, from preclinical to phase III. AIDS **15**(Suppl 5):S147–S158. http://dx.doi.org/10.1097/00002030-200100005-00018.
12. **Flynn NM, Forthal DN, Harro CD, Judson FN, Mayer KH, Para MF.** 2005. Placebo-controlled phase 3 trial of a recombinant glycoprotein 120 vaccine to prevent HIV-1 infection. J. Infect. Dis. **191:**654–665. http://dx.doi.org/10.1086/428404.
13. **Pitisuttithum P, Gilbert P, Gurwith M, Heyward W, Martin M, van Griensven F, Hu D, Tappero JW, Choopanya K.** 2006. Randomized, double-blind, placebo-controlled efficacy trial of a bivalent recombinant glycoprotein 120 HIV-1 vaccine among injection drug users in Bangkok, Thailand. J. Infect. Dis. **194:**1661–1671. http://dx.doi.org/10.1086/508748.
14. **Haynes BF, Gilbert PB, McElrath MJ, Zolla-Pazner S, Tomaras GD, Alam SM, Evans DT, Montefiori DC, Karnasuta C, Sutthent R, Liao HX, DeVico AL, Lewis GK, Williams C, Pinter A, Fong Y, Janes H, DeCamp A, Huang Y, Rao M, Billings E, Karasavvas N, Robb ML, Ngauy V, de Souza MS, Paris R, Ferrari G, Bailer RT, Soderberg KA, Andrews C, Berman PW, Frahm N, De Rosa SC, Alpert MD, Yates NL, Shen X, Koup RA, Pitisuttithum P, Kaewkungwal J, Nitayaphan S, Rerks-Ngarm S, Michael NL, Kim JH.** 2012. Immune-correlates analysis of an HIV-1 vaccine efficacy trial. N. Engl. J. Med. **366:**1275–1286. http://dx.doi.org/10.1056/NEJMoa1113425.
15. **Montefiori DC, Karnasuta C, Huang Y, Ahmed H, Gilbert P, de Souza MS, McLinden R, Tovanabutra S, Laurence-Chenine A, Sanders-Buell E, Moody MA, Bonsignori M, Ochsenbauer C, Kappes J, Tang H, Greene K, Gao H, LaBranche CC, Andrews C, Polonis VR, Rerks-Ngarm S, Pitisuttithum P, Nitayaphan S, Kaewkungwal J, Self SG, Berman PW, Francis D, Sinangil F, Lee C, Tartaglia J, Robb ML, Haynes BF, Michael NL, Kim JH.** 2012. Magnitude and breadth of the neutralizing antibody response in the RV144 and Vax003 HIV-1 vaccine efficacy trials. J. Infect. Dis. **206:**431–441. http://dx.doi.org/10.1093/infdis/jis367.
16. **Pancera M, Wyatt R.** 2005. Selective recognition of oligomeric HIV-1 primary isolate envelope glycoproteins by potently neutralizing ligands requires efficient precursor cleavage. Virology **332:**145–156. http://dx.doi.org/10.1016/j.virol.2004.10.042.
17. **Walker LM, Phogat SK, Chan-Hui PY, Wagner D, Phung P, Goss JL, Wrin T, Simek MD, Fling S, Mitcham JL, Lehrman JK, Priddy FH, Olsen OA, Frey SM, Hammond PW, Kaminsky S, Zamb T, Moyle M, Koff WC, Poignard P, Burton DR.** 2009. Broad and potent neutralizing antibodies from an African donor reveal a new HIV-1 vaccine target. Science **326:**285–289. http://dx.doi.org/10.1126/science.1178746.
18. **Walker LM, Huber M, Doores KJ, Falkowska E, Pejchal R, Julien JP, Wang SK, Ramos A, Chan-Hui PY, Moyle M, Mitcham JL, Hammond PW, Olsen OA, Phung P, Fling S, Wong CH, Phogat S, Wrin T, Simek MD, Koff WC, Wilson IA, Burton DR, Poignard P.** 2011. Broad neutralization coverage of HIV by multiple highly potent antibodies. Nature **477:**466–470. http://dx.doi.org/10.1038/nature10373.
19. **Lyumkis D, Julien JP, de Val N, Cupo A, Potter CS, Klasse PJ, Burton DR, Sanders RW, Moore JP, Carragher B, Wilson IA, Ward AB.** 2013. Cryo-EM structure of a fully glycosylated soluble cleaved HIV-1 envelope trimer. Science **342:**1484–1490. http://dx.doi.org/10.1126/science.1245627.
20. **Julien JP, Cupo A, Sok D, Stanfield RL, Lyumkis D, Deller MC, Klasse PJ, Burton DR, Sanders RW, Moore JP, Ward AB, Wilson IA.** 2013. Crystal structure of a soluble cleaved HIV-1 envelope trimer. Science **342:**1477–1483. http://dx.doi.org/10.1126/science.1245625.
21. **Bartesaghi A, Merk A, Borgnia MJ, Milne JL, Subramaniam S.** 2013. Prefusion structure of trimeric HIV-1 envelope glycoprotein determined by cryo-electron microscopy. Nat. Struct. Mol. Biol. **20:**1352–1357. http://dx.doi.org/10.1038/nsmb.2711.
22. **Kovacs JM, Nkolola JP, Peng H, Cheung A, Perry J, Miller CA, Seaman MS, Barouch DH, Chen B.** 2012. HIV-1 envelope trimer elicits more

potent neutralizing antibody responses than monomeric gp120. Proc. Natl. Acad. Sci. U. S. A. **109:**12111–12116. http://dx.doi.org/10.1073/pnas.1204533109.
23. **Yang X, Farzan M, Wyatt R, Sodroski J.** 2000. Characterization of stable, soluble trimers containing complete ectodomains of human immunodeficiency virus type 1 envelope glycoproteins. J. Virol. **74:**5716–5725. http://dx.doi.org/10.1128/JVI.74.12.5716-5725.2000.
24. **Zhang CW, Chishti Y, Hussey RE, Reinherz EL.** 2001. Expression, purification, and characterization of recombinant HIV gp140. The gp41 ectodomain of HIV or simian immunodeficiency virus is sufficient to maintain the retroviral envelope glycoprotein as a trimer. J. Biol. Chem. **276:**39577–39585. http://dx.doi.org/10.1074/jbc.M107147200.
25. **Sanders RW, Schiffner L, Master A, Kajumo F, Guo Y, Dragic T, Moore JP, Binley JM.** 2000. Variable-loop-deleted variants of the human immunodeficiency virus type 1 envelope glycoprotein can be stabilized by an intermolecular disulfide bond between the gp120 and gp41 subunits. J. Virol. **74:**5091–5100. http://dx.doi.org/10.1128/JVI.74.11.5091-5100.2000.
26. **Binley JM, Sanders RW, Clas B, Schuelke N, Master A, Guo Y, Kajumo F, Anselma DJ, Maddon PJ, Olson WC, Moore JP.** 2000. A recombinant human immunodeficiency virus type 1 envelope glycoprotein complex stabilized by an intermolecular disulfide bond between the gp120 and gp41 subunits is an antigenic mimic of the trimeric virion-associated structure. J. Virol. **74:**627–643. http://dx.doi.org/10.1128/JVI.74.2.627-643.2000.
27. **Schulke N, Vesanen MS, Sanders RW, Zhu P, Lu M, Anselma DJ, Villa AR, Parren PW, Binley JM, Roux KH, Maddon PJ, Moore JP, Olson WC.** 2002. Oligomeric and conformational properties of a proteolytically mature, disulfide-stabilized human immunodeficiency virus type 1 gp140 envelope glycoprotein. J. Virol. **76:**7760–7776. http://dx.doi.org/10.1128/JVI.76.15.7760-7776.2002.
28. **Sanders RW, Derking R, Cupo A, Julien JP, Yasmeen A, de Val N, Kim HJ, Blattner C, de la Pena AT, Korzun J, Golabek M, de Los Reyes K, Ketas TJ, van Gils MJ, King CR, Wilson IA, Ward AB, Klasse PJ, Moore JP.** 2013. A next-generation cleaved, soluble HIV-1 Env trimer, BG505 SOSIP. 664 gp140, expresses multiple epitopes for broadly neutralizing but not non-neutralizing antibodies. PLoS Pathog. **9:**e1003618. http://dx.doi.org/10.1371/journal.ppat.1003618.
29. **Binley JM, Sanders RW, Master A, Cayanan CS, Wiley CL, Schiffner L, Travis B, Kuhmann S, Burton DR, Hu SL, Olson WC, Moore JP.** 2002. Enhancing the proteolytic maturation of human immunodeficiency virus type 1 envelope glycoproteins. J. Virol. **76:**2606–2616. http://dx.doi.org/10.1128/JVI.76.6.2606-2616.2002.
30. **Beddows S, Schulke N, Kirschner M, Barnes K, Franti M, Michael E, Ketas T, Sanders RW, Maddon PJ, Olson WC, Moore JP.** 2005. Evaluating the immunogenicity of a disulfide-stabilized, cleaved, trimeric form of the envelope glycoprotein complex of human immunodeficiency virus type 1. J. Virol. **79:**8812–8827. http://dx.doi.org/10.1128/JVI.79.14.8812-8827.2005.
31. **Hu X, Saha P, Chen X, Kim D, Devarasetty M, Varadarajan R, Jin MM.** 2012. Cell surface assembly of HIV gp41 six-helix bundles for facile, quantitative measurements of hetero-oligomeric interactions. J. Am. Chem. Soc. **134:**14642–14645. http://dx.doi.org/10.1021/ja301099s.
32. **Chakrabarti BK, Pancera M, Phogat S, O'Dell S, McKee K, Guenaga J, Robinson J, Mascola J, Wyatt RT.** 2011. HIV type 1 Env precursor cleavage state affects recognition by both neutralizing and nonneutralizing gp41 antibodies. AIDS Res. Hum. Retroviruses **27:**877–887. http://dx.doi.org/10.1089/aid.2010.0281.
33. **Sattentau QJ, Moore JP.** 1995. Human immunodeficiency virus type 1 neutralization is determined by epitope exposure on the gp120 oligomer. J. Exp. Med. **182:**185–196. http://dx.doi.org/10.1084/jem.182.1.185.
34. **Grundner C, Mirzabekov T, Sodroski J, Wyatt R.** 2002. Solid-phase proteoliposomes containing human immunodeficiency virus envelope glycoproteins. J. Virol. **76:**3511–3521. http://dx.doi.org/10.1128/JVI.76.7.3511-3521.2002.
35. **Si Z, Cayabyab M, Sodroski J.** 2001. Envelope glycoprotein determinants of neutralization resistance in a simian-human immunodeficiency virus (SHIV-HXBc2P 3.2) derived by passage in monkeys. J. Virol. **75:**4208–4218. http://dx.doi.org/10.1128/JVI.75.9.4208-4218.2001.
36. **Leaman DP, Kinkead H, Zwick MB.** 2010. In-solution virus capture assay helps deconstruct heterogeneous antibody recognition of human immunodeficiency virus type 1. J. Virol. **84:**3382–3395. http://dx.doi.org/10.1128/JVI.02363-09.
37. **Bommakanti G, Citron MP, Hepler RW, Callahan C, Heidecker GJ, Najar TA, Lu X, Joyce JG, Shiver JW, Casimiro DR, ter Meulen J, Liang X, Varadarajan R.** 2010. Design of an HA2-based Escherichia coli expressed influenza immunogen that protects mice from pathogenic challenge. Proc. Natl. Acad. Sci. U. S. A. **107:**13701–13706. http://dx.doi.org/10.1073/pnas.1007465107.
38. **Bommakanti G, Lu X, Citron MP, Najar TA, Heidecker GJ, ter Meulen J, Varadarajan R, Liang X.** 2012. Design of Escherichia coli-expressed stalk domain immunogens of H1N1 hemagglutinin that protect mice from lethal challenge. J. Virol. **86:**13434–13444. http://dx.doi.org/10.1128/JVI.01429-12.
39. **Sanders RW, Vesanen M, Schuelke N, Master A, Schiffner L, Kalyanaraman R, Paluch M, Berkhout B, Maddon PJ, Olson WC, Lu M, Moore JP.** 2002. Stabilization of the soluble, cleaved, trimeric form of the envelope glycoprotein complex of human immunodeficiency virus type 1. J. Virol. **76:**8875–8889. http://dx.doi.org/10.1128/JVI.76.17.8875-8889.2002.
40. **Tran EE, Borgnia MJ, Kuybeda O, Schauder DM, Bartesaghi A, Frank GA, Sapiro G, Milne JL, Subramaniam S.** 2012. Structural mechanism of trimeric HIV-1 envelope glycoprotein activation. PLoS Pathog. **8:**e1002797. http://dx.doi.org/10.1371/journal.ppat.1002797.
41. **Liu J, Wang S, Hoxie JA, LaBranche CC, Lu M.** 2002. Mutations that destabilize the gp41 core are determinants for stabilizing the simian immunodeficiency virus-CPmac envelope glycoprotein complex. J. Biol. Chem. **277:**12891–12900. http://dx.doi.org/10.1074/jbc.M110315200.
42. **Moore JP, McKeating JA, Weiss RA, Sattentau QJ.** 1990. Dissociation of gp120 from HIV-1 virions induced by soluble CD4. Science **250:**1139–1142. http://dx.doi.org/10.1126/science.2251501.
43. **Earl PL, Broder CC, Doms RW, Moss B.** 1997. Epitope map of human immunodeficiency virus type 1 gp41 derived from 47 monoclonal antibodies produced by immunization with oligomeric envelope protein. J. Virol. **71:**2674–2684.
44. **Haim H, Strack B, Kassa A, Madani N, Wang L, Courter JR, Princiotto A, McGee K, Pacheco B, Seaman MS, Smith, AB, III, Sodroski J.** 2011. Contribution of intrinsic reactivity of the HIV-1 envelope glycoproteins to CD4-independent infection and global inhibitor sensitivity. PLoS Pathog. **7:**e1002101. http://dx.doi.org/10.1371/journal.ppat.1002101.
45. **Kang YK, Andjelic S, Binley JM, Crooks ET, Franti M, Iyer SP, Donovan GP, Dey AK, Zhu P, Roux KH, Durso RJ, Parsons TF, Maddon PJ, Moore JP, Olson WC.** 2009. Structural and immunogenicity studies of a cleaved, stabilized envelope trimer derived from subtype A HIV-1. Vaccine **27:**5120–5132. http://dx.doi.org/10.1016/j.vaccine.2009.06.037.
46. **Harris A, Borgnia MJ, Shi D, Bartesaghi A, He H, Pejchal R, Kang YK, Depetris R, Marozsan AJ, Sanders RW, Klasse PJ, Milne JL, Wilson IA, Olson WC, Moore JP, Subramaniam S.** 2011. Trimeric HIV-1 glycoprotein gp140 immunogens and native HIV-1 envelope glycoproteins display the same closed and open quaternary molecular architectures. Proc. Natl. Acad. Sci. U. S. A. **108:**11440–11445. http://dx.doi.org/10.1073/pnas.1101414108.
47. **Dimitrov AS, Jacobs A, Finnegan CM, Stiegler G, Katinger H, Blumenthal R.** 2007. Exposure of the membrane-proximal external region of HIV-1 gp41 in the course of HIV-1 envelope glycoprotein-mediated fusion. Biochemistry **46:**1398–1401. http://dx.doi.org/10.1021/bi062245f.
48. **Eckert DM, Kim PS.** 2001. Mechanisms of viral membrane fusion and its inhibition. Annu. Rev. Biochem. **70:**777–810. http://dx.doi.org/10.1146/annurev.biochem.70.1.777.
49. **Chakrabarti BK, Walker LM, Guenaga JF, Ghobbeh A, Poignard P, Burton DR, Wyatt RT.** 2011. Direct antibody access to the HIV-1 membrane-proximal external region positively correlates with neutralization sensitivity. J. Virol. **85:**8217–8226. http://dx.doi.org/10.1128/JVI.00756-11.
50. **Ruprecht CR, Krarup A, Reynell L, Mann AM, Brandenberg OF, Berlinger L, Abela IA, Regoes RR, Gunthard HF, Rusert P, Trkola A.** 2011. MPER-specific antibodies induce gp120 shedding and irreversibly neutralize HIV-1. J. Exp. Med. **208:**439–454. http://dx.doi.org/10.1084/jem.20101907.
51. **Doores KJ, Burton DR.** 2010. Variable loop glycan dependency of the broad and potent HIV-1-neutralizing antibodies PG9 and PG16. J. Virol. **84:**10510–10521. http://dx.doi.org/10.1128/JVI.00552-10.
52. **Liu J, Bartesaghi A, Borgnia MJ, Sapiro G, Subramaniam S.** 2008. Molecular architecture of native HIV-1 gp120 trimers. Nature **455:**109–113. http://dx.doi.org/10.1038/nature07159.
53. **Bajaj K, Madhusudhan MS, Adkar BV, Chakrabarti P, Ramakrishnan C, Sali A, Varadarajan R.** 2007. Stereochemical criteria for prediction of the effects of proline mutations on protein stability. PLoS Comput. Biol. **3:**e241. http://dx.doi.org/10.1371/journal.pcbi.0030241.

54. **Crooks ET, Tong T, Osawa K, Binley JM.** 2011. Enzyme digests eliminate nonfunctional Env from HIV-1 particle surfaces, leaving native Env trimers intact and viral infectivity unaffected. J. Virol. **85:**5825–5839. http://dx.doi.org/10.1128/JVI.00154-11.
55. **Wu SR, Loving R, Lindqvist B, Hebert H, Koeck PJ, Sjoberg M, Garoff H.** 2010. Single-particle cryoelectron microscopy analysis reveals the HIV-1 spike as a tripod structure. Proc. Natl. Acad. Sci. U. S. A. **107:**18844–18849. http://dx.doi.org/10.1073/pnas.1007227107.
56. **Pejchal R, Doores KJ, Walker LM, Khayat R, Huang PS, Wang SK, Stanfield RL, Julien JP, Ramos A, Crispin M, Depetris R, Katpally U, Marozsan A, Cupo A, Maloveste S, Liu Y, McBride R, Ito Y, Sanders RW, Ogohara C, Paulson JC, Feizi T, Scanlan CN, Wong CH, Moore JP, Olson WC, Ward AB, Poignard P, Schief WR, Burton DR, Wilson IA.** 2011. A potent and broad neutralizing antibody recognizes and penetrates the HIV glycan shield. Science **334:**1097–1103. http://dx.doi.org/10.1126/science.1213256.
57. **Bajaj K, Chakrabarti P, Varadarajan R.** 2005. Mutagenesis-based definitions and probes of residue burial in proteins. Proc. Natl. Acad. Sci. U. S. A. **102:**16221–16226. http://dx.doi.org/10.1073/pnas.0505089102.
58. **Chakrabarti BK, Feng Y, Sharma SK, McKee K, Karlsson Hedestam GB, Labranche CC, Montefiore DC, Mascola JR, Wyatt RT.** 2013. Robust neutralizing antibodies elicited by HIV-1 JRFL envelope glycoprotein trimers in nonhuman primates. J. Virol. **87:**13239–13251. http://dx.doi.org/10.1128/JVI.01247-13.